Elastic properties and atomic bonding character in metallic glasses

Tanguy Rouxel, Y. Yokoyama

Elastic properties and atomic bonding character in metallic glasses

T. Rouxel[1)] and Y. Yokoyama[2)]

[1)]*Institut de Physique de Rennes, IPR, UMR-CNRS 6251, Université de Rennes, campus de Beaulieu, 35042 Rennes cedex, France.*
[2)]*Cooperative Research and Development Center for Advanced Materials, Institute for Materials Research, Tohoku University, Sendai 980-8577, Japan.*

The elastic properties of glasses from different metallic systems were studied in the light of the atomic packing density and bonding character. We found that the electronegativity mismatch (Δe^-) between the host- and the major solute - elements provides a plausible explanation to the large variation observed for Poisson's ratio (ν) among metallic glasses (MGs) (from 0.28 for Fe-based to 0.43 for Pd-based MGs) notwithstanding a similar atomic packing efficiency (C_g). Besides, it is found that ductile MGs correspond to Δe^- smaller than 0.5 and to a relatively steep atomic potential well. Ductility is thus favored in MGs exhibiting a weak bond directionality in average and opposing a strong resistance to volume change.

I. INTRODUCTION

In comparison with oxide glasses, MGs are characterized by larger ν and C_g coefficients[1,2]. Nevertheless, while a monotonic increase of ν with C_g was reported for oxide glasses[3,4] the situation seems much more complicated for MGs (Fig.1). Indeed as far as ionic and/or covalent bonding are concerned, the atomic network connectivity has a direct incidence on C_g (the better the connectivity is, the smaller ν becomes), and the average atomic coordination for covalent glasses (chalcogenides) and the number of bridging anion per cation-centered tetrahedron (silicates) are relevant structural parameters to discuss the network connectivity. In the case of MGs the weak atomic bonding directionality and the lack of interconnected 1D-, 2D-, or 3D-structural units prevent from a simple analogy. However MGs are obtained from metalloids and transition metals with significantly contrasted physical and chemical properties, so that as soon as different chemical systems are under scrutiny large changes in the electronic bonding characteristics are observed. Here we focused on the Δe^- and on the parameters (U_o, m, n) of an empirical Lennard-Jones (LJ) type expression for the cohesion potential. While Δe^- is a measure of the bond strength and directionality, LJ parameters reflect the sensitivity to a variation of the distance between atoms or structural units (clusters), and are related to the material stiffness. Combining Δe^- and LJ parameters open new perspectives to promote ductility among MGs and to assess the plastic flow mechanism. In what follows, previously published elasticity and density data for MGs belonging to various chemical systems[1,5-9], including Cu-, Ni-, Pd-, Pt-, Fe-, Zr-, Ti-, Mg-, Ca-, La-, Ce-based glasses, were used to get insight into the relationship between the elastic properties, the atomic packing efficiency, and the atomic bonding character.

II. POISSON'S RATIO, ATOMIC PACKING DENSITY, AND ELECTRONEGATIVITY

In order to allow for a straightforward comparison with previous reports on oxide glasses, the atomic packing density is defined as the ratio between the minimum theoretical volume occupied by the atoms and the corresponding effective volume of glass

$$C_g = \rho \Sigma f_i V_i / (\Sigma f_i M_i) \quad (1)$$

with for the i^{th} constituent: $V_i = 4/3 \pi \mathcal{N} r_i^3$, where ρ is the specific mass, $\mathcal{N}$ is Avogadro number, r_i is the metallic radius[10-12] (i.e. half the shortest distance between two atoms in the pure metal), f_i is the molar fraction and M_i is the molar mass. The use of the experimental values for the interatomic distance[11,13] to calculate C_g instead of the classical values for pure metals was found to have only a minor incidence on C_g in cases actual interatomic distances were available. For instance the values reported by Egami et al.[11] and Inoue[12] were found to alter the calculated C_g values by less than 5% in all studied cases. For example, for $Cu_{50}Zr_{50}$ and $Ni_{80}P_{20}$ glasses, accounting for the actual average interatomic distances changes C_g from 0.737 to 0.723 (-2%), and from 0.701 to 0.725 (+4%). Interestingly ν is mostly larger for MGs than expected by means of a simple rule of mixture from the properties of the constituting elements. This suggests a better packing efficiency in average, in agreement with structural models and experimental observations. However, in contrast with silicate glasses where a one to one relationship was found between ν and C_g ($\nu = 1/2\text{-}1/(7.2C_g)$)[3], there is no straightforward correlation in the case of MGs. For instance, Fe-, Ti-, and Pd-based MGs have roughly the same C_g (~0.63-0.65) but their ν values spread from 0.28 to 0.43. A general trend among materials and structures which proved to be scale-independent is that ν decreases as the connectivity increases[14]. This rules holds for macrostructures such as construction frames or cellular systems, as well as for atomic-scale structures. In ionocovalent solids, 2D and 3D atomic networks are favored thanks to the strength and the directionality of the bonding. It is thus inferred that non transition metal host elements such as Ce, Ca, and Mg, develop more directional bonding through better localized f (for Ce) and sp (Ca,Mg) electrons giving rise to a relatively small ν. Some evidence for this is provided by the electronegativity difference between the host and the two major secondary elements (Table I), and the remarkable correlation found between ν and Δe^- (Fig. 2) which suggests that ν primarily depends on the bond directionality and connectivity rather than on C_g. Besides, this correlation provides an explanation for the variation of ν within a given MG chemical system or for isostructural monoconstituent oxide glasses. For instance in Zr-based glasses, ν is found to increase with the Al content in the ZrAlCu system, and Δe^-~0.28 and 0.29 for the Zr-Al and Cu-Al pairs respectivily, to be compared with 0.57 for the Cu-Zr pair. In the case of "tetrahedral" oxide glasses such as a-SiO_2, a-GeO_2, a-TeO_2, or "trihedral" glasses such as a-As_2O_3, a-B_2O_3, and a-P_2O_5[15] (where the double P=O bond confers a $(P{=}O)O_{3/2}$ trihedral structure) the change in ν which was not elucidated so far can also be interpreted in the light of the Δe^- variation. Note that for MGs ν provides an indication of the ductility that can be expected. Metallic glasses with ν>0.32 usually exhibit significant ductility at room temperature[16,17]. A molecular dynamic study of amorphous solids using a two-body LJ potential to model atomic interactions with coordination numbers between 7 and 12 also corroborated this result and came to the conclusion that ductility is favored by reducing the covalent character[18]. ν>0.32 corresponds to Δe^-<0.5. In the case of Pd- and Pt-based MGs, Δe^- is as low as 0.01 and 0.09 respectively. For Fe-, Ce-, and Ca-based MGs which are known to behave in a brittle manner, Δe^- is typically larger than 0.5. In Fe-based glasses containing C and Cr, C is expected to react with Cr due to a large enthalpy of mixing[19] (in absolute value) and Δe^-(Cr-C)=0.89, and Δe^-(Fe-C)=0.72. For Ce-based MGs, containing Ni, Al and Cu, Ce preferentially reacts with Al (Δe^-(Ce-Al)=0.49) and Δe^-(Ce-Cu)≈Δe^-(Ce-Ni)=0.79. For Ca-based MGs containing Mg and Cu, Ca is supposed to react with Cu ($|\Delta H_{mixing}(Ca,Cu)| > |\Delta H_{mixing}(Ca,Mg)|$) and Δe^-(Ca-Cu)=0.9. Recalling that ν scales with K/μ where K and μ are bulk and shear elastic moduli respectively ($\nu = (3K/\mu\text{-}2)/(6K/\mu + 2)$), as ν increases, ductility is enhanced, and isochoric shear flow prevails over volume changes. While the Δe^- parameter shows up as a measure of the ease for shear, i.e. for relative displacement of atoms or groups of atoms with respect to each other along paths normal to center-to-center direction, the shape, and especially the steepness of the interatomic potential comes into play as soon as local volume changes - or variation of center-to-center distances - are considered.

III. ELASTIC PROPERTIES AND DISSOCIATION ENERGY

In what follows we use a classical derivation of an elastic modulus from an empirical central force potential[20-22], here a LJ potential. The metallic bonding is essentially collective and there is no such thing as an isolated "metallic bond", so that instead of looking for a rough estimation of the cohesive energy from the atomic pair interaction and a speculated and mostly irrelevant local coordination, an isotropic potential is considered. A volume density of energy, $<U_o>/<V_o>$, is estimated from the energy content $<U_o>$ and the corresponding volume $<V_o>$, where $<V_o>$ is the molar volume of a gram atom, that is an equivalent atom accounting for the stoichiometric composition of the alloy

$$<V_o>=\sum_i \frac{f_i M_i}{\rho} \qquad (2)$$

The external work to produce a small volume change in a reversible manner is expressed as

$$\Delta W = \int_{V_o}^{V} -P dV = \int_{V_o}^{V} \frac{K\Delta V}{V_o} dV = K\frac{(\Delta[V])^2}{2V_o} \qquad (3)$$

where P is the hydrostatic pressure, K is the bulk modulus and ΔV the volume change.

Equating the internal energy change, ΔU, to ΔW and remembering that at equilibrium (i.e. for $V=V_o$) $\left.\frac{\partial U}{\partial V}\right|_{V_o} = 0$ leads to

$$K = V_o \left.\frac{\partial^2 U}{\partial V^2}\right|_{V_o} \qquad (4)$$

Further considering a Lennard-Jones (LJ) type potential for the internal potential of the system

$$U(r) = \frac{nU_o}{m-n}\left[\left(\frac{r_o}{r}\right)^m - \frac{m}{n}\left(\frac{r_o}{r}\right)^n\right] \qquad (5)$$

where U(r) is not to be understood as an interatomic pair potential but as a central force potential aimed at describing essentially radial interactions between structural units (such as inter-cluster interactions), the classical expression known as the 1st Grüneisen's rule is obtained[20]

$$K = \frac{mnU_o}{9V_o} \qquad (6)$$

It is noteworthy that this expression stems from the assumption that the cohesive energy can be differentiated with respect to the atomic volume. In the case of a pair-interaction potential, U_o is the energy required to suppress the bond and the cohesive energy of the system is half the bonding energy for each bond and accounts for the local coordination number, Z

$$<U_o>=ZU_o/2 \qquad (7)$$

By analogy, considering a representative volume $<V_o>$ we may write

$$K = \frac{2mn < U_o >}{9 < V_o >} \qquad (8)$$

where $<U_o>$ is the molar dissociation energy and was estimated from existing thermochemistry data[10,19] for the elements constituting the studied glasses. In eq. (8) the 2/9 pre-factor can hardly be given any physical meaning in the cases of glasses inasmuch as fine details of the atomic network structure are unknown and long-range interactions are disregarded. However some new insight into the structure and the peculiarities of MGs from different chemical systems can be gained by comparing the (m,n) values deriving from the experimental K values, $<U_o>$ and the molar volume $<V_o>$.

In the case of a binary system, $<U_o>$ is expressed as

$$<U_o> = x\Delta H_{at}(A,g)+y\Delta H_{at}(B,g)-\Delta H_{mixing}(A_xB_y) \qquad (9)$$

$<U_o>$ is the energy (standard pressure) necessary to obtained separate gaseous atoms from the solid material (a gram atom is considered: x+y=1), according to the schematic drawing shown in Fig. 4. Note that the enthalpy of mixing is rarely known for multi-constituent metallic systems. Furthermore it might not represent the situation in amorphous systems, inasmuch the glassy network exhibits some peculiar structural features such as chemical segregation, clustering etc. Nevertheless, in most cases, the enthalpy of mixture is much smaller than the atomization enthalpy in absolute values. The atomization (sublimation) enthalpy is typically of several hundreds kJ/mol (605, 326, 431, and 338 for Zr, Al, Ni and Cu respectively), whereas the enthalpy of mixing is less than the enthalpy of formation (about -34 kJ/mol for ZrCu, -57 kJ/mol for PdSi, -30 kJ/mol for Ni_5P…) and is of few tens kJ/mol. Therefore in what follows, as long as different chemical systems are under scrutiny and for sake of comparison, the dissociation energy of a multi-constituent glass will be written

$$<U_o> = \sum_i f_i \, \Delta H^i_{atomisation} \qquad (10)$$

where f_i is the atomic fraction of the i^{th} constituent.

The dissociation energy, the molar volumes, and the corresponding volume density of energy of series of metallic glasses from different chemical systems were calculated. The global trend for glass is an increase of T_g with $<U_o>$ (Fig. 4), as the binding energy of pure substances scales with the melting point. However, as soon as a particular system is under scrutiny, somewhat unexpected tendencies are observed, as is the case for in Zr-based glass systems, where $<U_o>$ may increase while T_g decreases. This observation supports the hypothesis of an heterogeneous glass network structure where T_g is primarily governed by a glassy sub-network having a composition differing from the stoichiometric one. For example, the addition of aluminum to glasses from the (Zr,Cu) system results in an important deviation from random mixing, with an excess of aluminum at the vicinity of zirconium leading to (Zr,Al) rich regions, embedded in a (Zr,Cu) rich matrix depleted in aluminum. While the increase in $<U_o>$ with the Zr/Cu ratio is somewhat consistent with Zr having a higher melting point (T_m=2128 K) than Cu (T_m=1358 K), the decrease of T_g (from 706 to 671 K as the composition changes from $Zr_{50}Cu_{40}Al_{10}$ to $Zr_{60}Cu_{30}Al_{10}$) might be related to the deviation from random mixing and to the behavior of the percolating phase if any.

K is plotted as a function of $<U_o>/<V_o>$ in Fig. 5. It is noteworthy that using the density of the pure constituent for an ab-initio calculation (open symbols) in lieu of the density of the glass to estimate $<V_o>$ (closed symbols) has only little - as for Pt, Pd and Ni-based glasses - or no incidence - other studied systems - on the volume density of energy. The bulk modulus of glasses belonging to a specific system depends almost linearly on the volume density of energy calculated for the given system. However the slope of the linear interpolation depends much on the chemical

composition. The corresponding (m,n) exponents are given in Table I using the m=2n approximation, thus following previously published analysis on similar metallic systems[23,24]. The larger the (m,n) values are and the steeper the potential well is. Most glasses investigated in this study are associated to $m_xn \approx 10\text{-}11.5$. The exponents are found to scale quite well with ν. Pd- and Pt-based glasses, with $m_xn > 16$, exhibit ν values above 0.38, whereas La- and Ce-based glasses are associated to m_xn values smaller than 10, and ν smaller than 0.29. of 0.28 and 0.24 respectively. There is also a relatively good agreement (but for Zr and Mg) between the m_xn product and the ν value of the pure constituent (Table I): 0.38 and 0.39 for Pt and Pd respectively, and 0.24 and 0.28 for Ce and La respectively. This is indeed what could be anticipated from changes in the potential steepness. A steep potential for the material compressibility leaves little room for changes in the inter-unit distance (a structural unit here can be either an atom, a group of atoms representative of the glass stoichiometry, or a cluster with a peculiar chemical composition, depending on the way the glass behave under mechanical loading at the atomic scale) so that shear is expected to predominate, in agreement with large ν values. On the contrary for a relatively small m_xn product, the structural units might move each with respect to the others with center to center distance variations and local volume contraction or expansion. Different atomic clusters may exist that also possess high local packing efficiency and may act as such structural units: The capped trigonal prism, and a coordination number of 9, and icosahedra, with a coordination number of 12, are two such solute-centered clusters that are known to exist in metallic glass structures[25,26].

The change in the composition for a given system leads to a progressive shift from a given interpolation line to another in Fig. 5. For instance in the Cu-based system (see the insert in Fig. 5), as the zirconium content increases, K decreases (consistently with the fact that K(Cu)=140 GPa>K(Zr)=71 GPa) from about 117 to 100, so that the data points are seen to meet the data corresponding to the Zr-based glasses. In the ZrCu system, the packing density increases with increasing the Cu content and plastic deformation becomes more difficult since a local structural change accompanied by a local volume expansion is needed for shear deformation to proceed. This is corroborated by the decrease of ν ($\nu(Cu_{46}Zr_{54})=0.391$, $\nu(Cu_{50}Zr_{50})=0.36$, $\nu(Cu_{65}Zr_{35})=0.33$)[27] and the increase of the "m_xn" product with an increase of the Cu content. In fact the strong sensitivity of the LJ potential to the chemical system prevents from having a universal relationship between K and $\langle U_o \rangle / \langle V_o \rangle$ allowing for an ab-initio estimation of the elastic modulus. The same situation was already observed in the case of oxide glasses[4] and reveals some structural complexity. It is noteworthy in this latter case that whatever the chemical system, ν and C_g are significantly smaller than for the metallic glasses, and so is the m_xn product. C_g for silicate glasses is typically between 0.4 and 0.55, and $K/(\langle U_o \rangle / \langle V_o \rangle) \approx 3/4$, so that $m_xn \approx 3.4$, consistently with the fact that oxide glasses are much more brittle than the metallic ones, and undergo significant volume change under mechanical loading (for instance pure SiO_2 glass, with $\nu \approx 0.15$, can experience up to 20 % densification under hydrostatic loading).

While Δe^- provides an indication for the bond directionality - a property which is clearly related to the resistance to shear deformation - and is reflected in the three dimensional picture of the energy landscape, the two dimensional cross section depicted by the center to center potential profile determines the resistance to compression and stretching, and hence to volume change. Thus, the present analysis opens the perspective of possible correlations between structural characteristics such as Δe^- and the potential well parameters, and the constitutive laws for plastic flow or for densification.

IV. ELASTIC MODULI AND GLASS TRANSITION RANGE

Young's modulus (E) and T_g data for series of metallic glasses, taken from previously published papers[1,5,13,28,29], are plotted in Fig. 6. These data are discussed in the light of the atomic

packing densities, which are given as a function of Poisson's ratio (ν) in Fig. 1, and of the energy content, which is given as a function of T_g in Fig. 4. To get some insight into a possible E-T_g correlation, it is interesting to compare i) Metallic glasses with other glasses (silicates, chalcogenides…); ii) metallic glasses from different chemical systems; and iii) metallic glasses with different compositions from a given metallic system. In comparison with non-metallic glasses, metallic glasses are advantaged by mostly larger elastic moduli than oxide, as large as those of the oxynitride glasses although their T_g is usually much smaller (Fig. 4). Metallic glasses being adavantaged by a significantly larger atomic packing efficieny, this comparison provides evidence for the effect of the atomic packing density on the elastic moduli. It is also noteworthy that there is a global increase of T_g of the different glasses with the energy content which increases almost monotonically in the following order: chalcogenide<metallic<silicates<silicon oxynitrides<pure silica glass. As far as metallic glasses from different systems are concerned a general increase of E with T_g is observed, with the lower values being observed for Ce- and Ca-based glasses while Fe- and W-based glasses are the stiffest and the most refractory. Nevertheless there is no one-to-one relationship and for a given E value, the transition temperature shift can be as high as 300 K. Interestingly a similar observation can be made when bulk modulus is plotted as a function of the melting temperature, as was done by Tanaka et al.[29]. In this case, for a given value of bulk modulus - let us take 150 GPa for instance - the temperature interval where metallic and intermetallic materials melt extends from 1000 (PdCuNiP glass) to 2500 K (Niobium) (Fig. 5 in ref. [29]). Indeed E being given in Pa, i.e. in J/m^3, whereas T_g is comparable with an energy, the atomic packing density (C_g) needs to be invoked to describe the energy density of the network. Considering the horizontal segments labeled 1, 2 and 3 in Fig. 6, it turns out that C_g decreases along these segments for compositions belonging to the same chemical system as illustrated by the insert in Fig. 6. Comparing metallic glasses from different chemical systems remains difficult though, probably because an average packing efficiency (Eq. 1) doesn't take into account the spatial distribution of the packing density[26], as well as the incidence of the local packing geometry and coordination[25]. For instance, in spite of a mostly smaller C_g for Pt-based glasses than for Cu-based glasses (Fig. 1), Pt-glasses along segment labeled 2 in Fig. 6 have about the same Young's modulus. With a smaller C_g and a lower energy content (Figs. 1,4), Young's modulus (Fig. 6) and bulk modulus (Fig. 5) of Pd-based glasses are also surprisingly high. The calculation of the electronic structure of the characteristic clusters occurring in Pd-Ni-P glasses (system of concern in the present analysis) revealed dominantly covalent bonding at phosphorus atoms[30]. The high stability of Pd-based glasses would find its source in this covalent nature of the bonding at phosphorus sites associated with the existence of more compliant inter-cluster regions enriched in palladium and nickel. These latter regions promote shear deformation and a large ν value, while the covalent bonds might be responsible for the relatively low C_g.

V. CONCLUSION

In conclusion, metallic glasses exhibits neither one to one relationship between C_g and ν, (as for silicate glasses) nor between elastic moduli and T_g. Nevertheless, ν is found to increase as the difference in electronegativity between the host metal and the major solute elements decreases, so that a ductile behavior is expected for $\Delta e^- < 0.5$ (corresponding to $\nu > 0.33$). This correlation also holds for monoconstituent oxide glasses and hence provides an explanation to the variation of ν observed for seemingly "isostructural" glasses. The relationship between K and the volume density of energy $\langle U_o \rangle / \langle V_o \rangle$ as estimated for series of glasses from thermochemistry data was modeled by means of a LJ type potential function. Largest LJ exponent values were observed for Pd- and Pt-based glasses, and smaller ones for Ce- and La-based glasses. Most glasses (Cu-, Zr-, Ti-, Fe-,…) exhibit similar values, much larger than those reported for oxide glasses. This is consistent with the

fact that the efficient atomic packing in MGs leaves little room for volume change in comparison with oxide glasses, and is conducive to isochoric shear flow, inasmuch as Δe^- is small.

References:

1. W.H. Wang, The elastic properties, elastic models and elastic perspectives of metallic glasses. Progress Mat. Sci. **57**, 487-656 (2012).
2. D.B. Miracle, and W.S. Sanders, The influence of efficient atomic packing on the constitution of metallic glasses. Phil. Mag. **83**, 2409-2428 (2003).
3. A. Makishima, and J.D. Mackenzie, Calculation of Bulk Modulus, Shear. Modulus and Poisson's Ratio of Glass. J. Non-Cryst. Sol., **17**, 147-157 (1975).
4. T. Rouxel, Elastic Properties and Short-to Medium-Range Order in Glasses. J. Am. Ceram. Soc. **90**, 3019-3039 (2007).
5. Y. Yokoyama, and A. Inoue, Compositional Dependence of Thermal and Mechanical Properties of Quaternary Zr-Cu-Ni-Al Bulk Glassy Alloys. Mat. Trans. **48**, 1282-1287 (2007).
6. N. Mattern, J. Bednarcik, S. Pauly, G. Wang, J. Das, and J. Eckert, Structural evolution of Cu–Zr metallic glasses under tension. Acta Mater. **57**, 4133-4139 (2009).
7. K.W. Park, J. Jang, M. Wakeda, Y. Shibutani, and J. Lee, Atomic packing density and its influence on the properties of Cu–Zr amorphous alloys. Scripta Mater. **57**, 805-808 (2007).
8. C.C. Yuan, and X.K. Xi, On the correlation of Young's modulus and the fracture strength of metallic glasses. J. App. Phys**. 109,** 033515 (2011).
9. R. Tarumi, M. Hirao, T. Ichitsubo, E. Matsubara, J. Saida, and H. Kato, Low-temperature acoustic properties and quasiharmonic analysis for Cu-based bulk metallic glasses. Phys. Rev. B, **76**, 104206 (2007).
10. Handbook of Chemistry and Physics, Ed. D. R. Lide, 86th Edition, Pub. Taylor & Francis (2005-2006).
11. T. Egami, and Y. Waseda, Atomic size effect on the formability of metallic glasses. J. non-Cryst. Sol. **64**, 113-134 (1984).
12. A. Inoue, Stabilization of metallic supercooled liquid and bulk amorphous alloys. Acta Mater**. 48**, 279-306 (2000).
13. R.H. Schumm, National Bureau of Standards (USA) Technical Notes 270-1 to 270-8 (1973).
14. G.N. Greaves, A.L. Greer, R.S. Lakes, and T. Rouxel. Poisson's ratio and modern materials. Nature Mat**. 10**, 823-837 (2011).
15. B. Bridge, N.D. Patel, D.N. Waters. On the elastic constants and structure of the pure inorganic oxide glasses. Phys. Sta. Sol. (a) **77**, 655-668 (1983).
16. X.J. Gu, S.J. Poon, G.J. Shiflet, and M. Widom, Ductility improvement of amorphous steels: Roles of shear modulus and electronic structure. Acta Mat. **56**, 88-94 (2008).
17. S.V. Madge, D.V. Louzguine-Luzgin, J.J. Lewandowski, and A.L. Greer, Toughness, extrinsic effects and Poisson's ratio of bulk metallic glasses. Acta Mater. **60**, 4800-4809 (2012).
18. Y. Shi, J. Luo, F. Yuan, and L. Huang, Intrinsic ductility of glassy solids. J. App. Phys., **115**, 043528 (2014).
19. F.R. De Boer, "Cohesion in metals - Transition metal alloys", F.R. de Boer and D.G. Pettifor Ed., Elsevier Science pub. (1989).
20. E. Grüneisen, 1st rule in "Physical Properties of Solid Materials", Ed. C. Zwikker, Willey Interscience, New-York, p.90 (1954).
21. A. Makishima, and J.D. Mackenzie, Direct calculation of Young's modulus of glass. J. Non-Cryst. Sol., **12**, 35-45 (1973).
22. S. Inaba, et al. Young's Modulus and Compositional Parameters of Oxide Glasses. J. Am. Ceram. Soc. **82**, 3501-3507 (1999).
23. M. Wakeda, Y. Shibutani, S. Ogata, and J. Park, Relationship between local geometrical factors and mechanical properties for Cu–Zr amorphous alloys. Intermetallics **15**, 139-144 (2007).

24. T. Lin, X.F. Bian, J. Jiang, Relation between calculated Lennard-Jones potential and thermal stability of Cu-based bulk metallic glasses. Phys. Lett. A **353**, 497-499 (2006).
25. D.B. Miracle, A structural model for metallic glasses. Nature Mat. **3**, 697-701 (2004).
26. A. Hirata, and Y. Hirotsu, Structure Analyses of Fe-based Metallic Glasses by Electron Diffraction. Mat. **3**, 5263-5273 (2010).
27. H.W. Sheng, W.K. Luo, F.M. Alamgir, J.M. Bai, and E. Ma, Atomic packing density and short-to-medium range order in metallic glasses. Nature **439**, 419-425 (2006).
28. W.H. Wang, Elastic moduli and behaviors of metallic glasses. J. Non-Cryst Sol. **351**, 1481-1485 (2005).
29. K. Tanaka, T. Ichitsubo, and E. Matsubara, Elasticity and anelasticity of metallic glass near the glass transition temperature. Mat. Sci. Engng. **A 442**, 278-282 (2006).
30. T. Takeuchi et al., Electronic Structure and Stability of the Pd-Ni-P Bulk Metallic Glass. Mat. Trans. **48**, 1292-1298 (2007).

Acknowledgments:

The European Research Council is greatly acknowledged for the Advanced Grant 320506 (DAMREG) of the 7th framework program “Ideas”. This work was initiated during a study leave at IMR-Tohoku University (Sendai), thanks to Prof. A. Makino.

Correspondence and requests for materials should be addressed to Tanguy ROUXEL (e-mail: tanguy.rouxel@univ-rennes1.fr)

TABLE I. (m,n) power law exponents of the L-J potential as estimated by linear interpolation of the K vesrus $<U_o>/<V_o>$ data (Fig. 5), and electronegativity (Pauling). Data obtained on the pure substances from their bulk modulus and density are given for comparison[10]. Following earlier investigators on similar materials, the m=2n approximation is used.

	Cu-based	Ni-based	Pd-based	Pt-based	Fe-based	Zr-based	Ti-based	Mg-based	Ca-based	La-based	Ce-based
m,n - Glasses	4.82, 2.41	4.85, 2.42	5.92, 2.96	5.74, 2.87	4.69, 2.35	4.71, 2.36	4.58, 2.29	4.8, 2.4	4.47, 2.24	4, 2	3.46, 1.73
m,n - host element	5.16, 2.58	5, 2.5	6.2, 3.1	5.78, 2.89	5.14, 2.57	3.85, 1.92	4.73, 2.37	6.28, 3.14	4.77, 2.39	3.63, 1.82	3.13, 1.57
ν (host element)	0.34	0.31	0.39	0.38	0.29	0.34	0.32	0.29	0.31	0.28	0.24
□□□ctronegativity, e_i, (host element)	1.9	1.91	2.2	2.28	1.83	1.33	1.54	1.31	1	1.1	1.12
$\Delta e^- = \lvert \square_{\square} \square \square_{\square} \rvert$ j^{th} □□□□□□□□y element in brackets	0.57 (Zr) 0.29 (Al)	0.28 (P) 0.28(Zr)	0.01 (P) 0.3 (Cu)	0.09 (P) 0.37 (Ni)	0.72 (C) 0.17 (Cr)	0.57 (Cu) 0.28 (Al)	0.21 (Zr) 0.03 (Be)	0.6 (Ni) 0.59 (Cu)	0.31 (Mg) 0.9 (Cu)	0.8 (Cu) 0.51 (Al)	0.79 (Ni) 0.78 (Cu)

Figure captions:

FIG. 1. Poisson's ratio as a function of the atomic packing density (Eq. (1)).

FIG. 2. Poisson's ratio as a function of the electronegativity mismatch between the host metal and the major secondary solute elements (horizontal error bars show the interval with the two major solutes).

FIG. 3. Schematic drawing of the enthalpy contributions which come into play in the determination of the dissociation energy $<U_o>$ in the case of a binary A_xB_y alloy.

FIG. 4. Dissociation energy $<U_o>$ as estimated from thermochemistry data as a function of T_g. Data on chalcogenide, phosphate, silicate, and oxynitride glasses were extracted from ref. [3].

FIG. 5. Bulk modulus (K) as a function of the volume density of energy. Open symbols correspond to the volume density of energy obtained using the molar volume as calculated from the density of the individual constituents and their atomic fraction (rule of mixture), while the closed symbols derive from the molar volume of the glass as obtained from the density of the glass.

FIG. 6. Young's modulus as a function of T_g for metallic glasses from different chemical systems. Data from refs. [1,3,9,13,28,29].

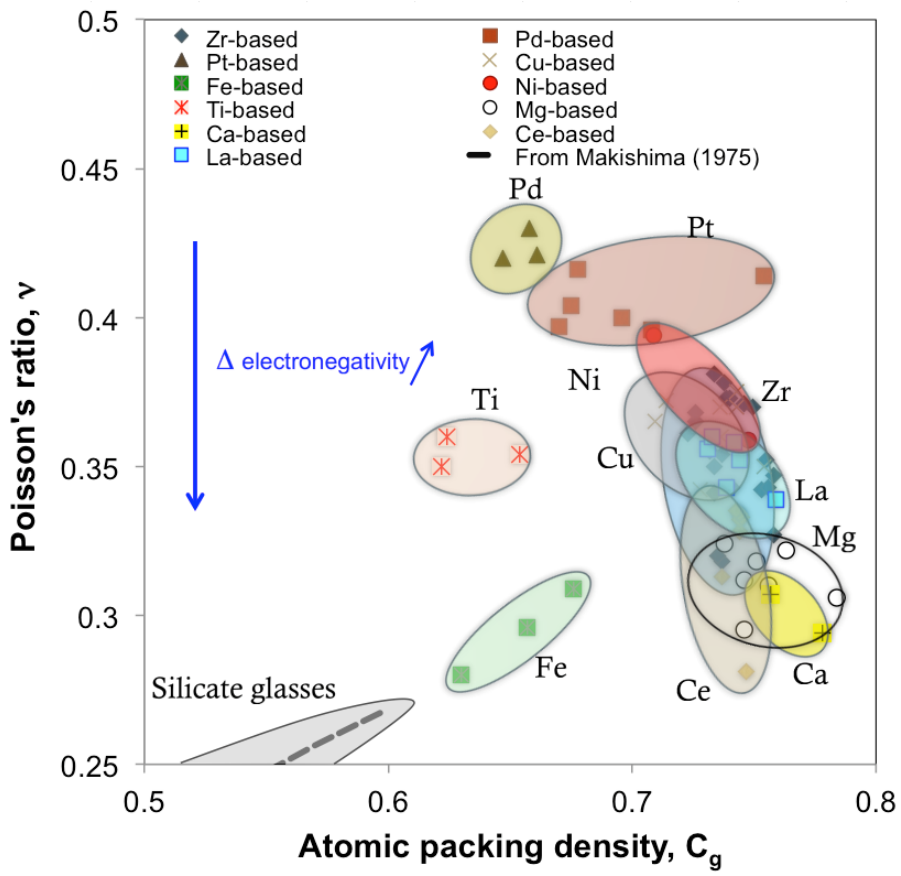
Zr-based
Pt-based
Fe-based
Ti-based
Ca-based
La-based
Pd-based
Cu-based
Ni-based
Mg-based
Ce-based
From Makishima (1975)
Pd
Pt
Ni
Zr
Ti
Cu
La
Mg
Fe
Ca
Ce
Silicate glasses
Δ electronegativity
Poisson's ratio, ν
Atomic packing density, C_g
0.5
0.45
0.4
0.35
0.3
0.25
0.5
0.6
0.7
0.8

FIG. 1

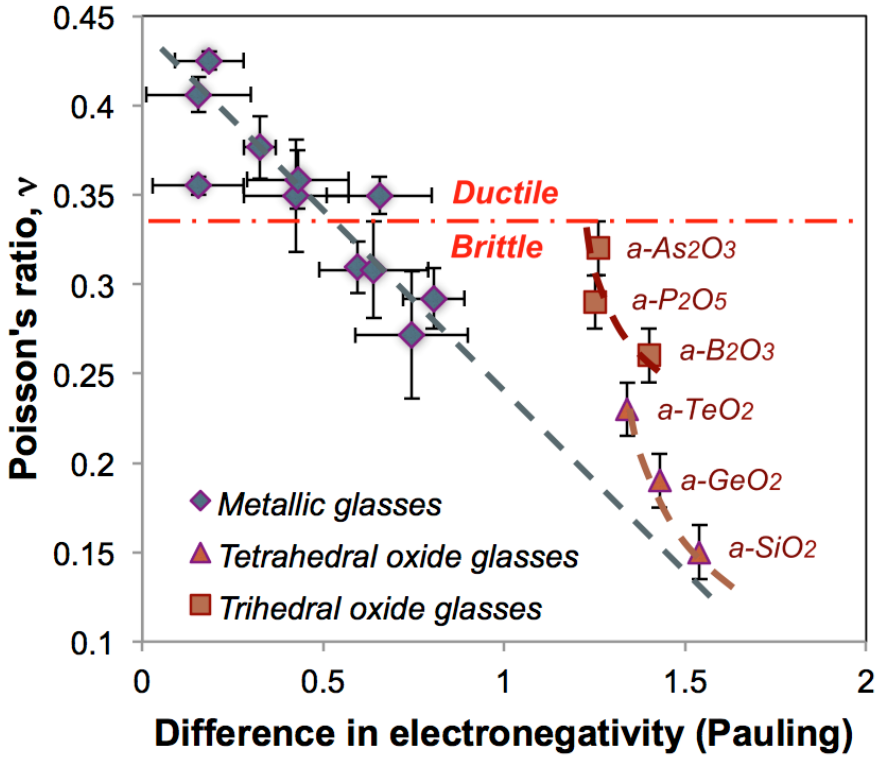
Ductile
Brittle
a-As2O3
a-P2O5
a-B2O3
a-TeO2
a-GeO2
a-SiO2
Metallic glasses
Tetrahedral oxide glasses
Trihedral oxide glasses
Poisson's ratio, ν
Difference in electronegativity (Pauling)
0.45
0.4
0.35
0.3
0.25
0.2
0.15
0.1
0
0.5
1
1.5
2

FIG. 2

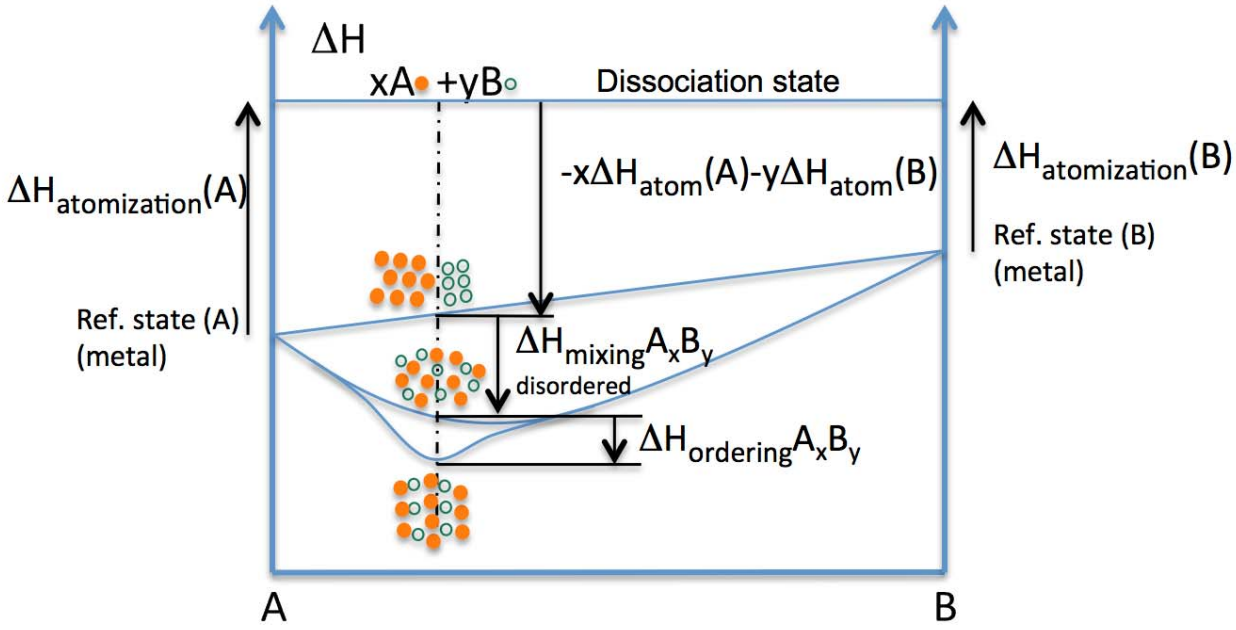
ΔH
xA +yB
Dissociation state
ΔH atomization(A)
-xΔH atom(A)-yΔH atom(B)
ΔH atomization(B)
Ref. state (B)
(metal)
Ref. state (A)
(metal)
ΔH mixing AxBy
disordered
ΔH ordering AxBy
A
B

FIG. 3

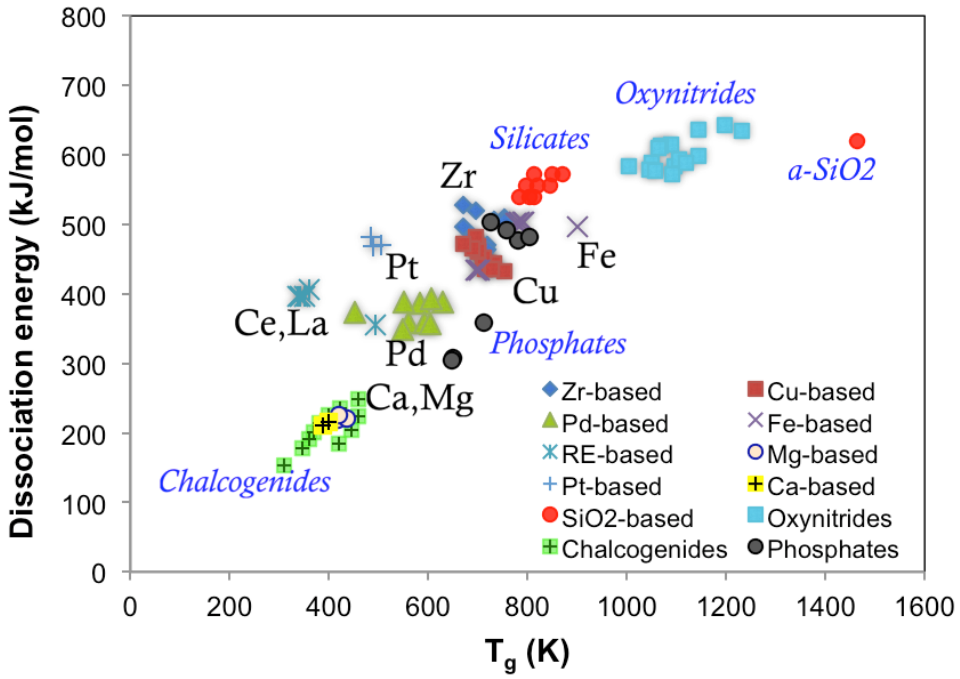
Dissociation energy (kJ/mol)
Tg (K)
0
100
200
300
400
500
600
700
800
0
200
400
600
800
1000
1200
1400
1600
Oxynitrides
Silicates
a-SiO2
Zr
Fe
Pt
Cu
Ce,La
Pd
Phosphates
Ca,Mg
Chalcogenides
Zr-based
Cu-based
Pd-based
Fe-based
RE-based
Mg-based
Pt-based
Ca-based
SiO2-based
Oxynitrides
Chalcogenides
Phosphates

FIG. 4

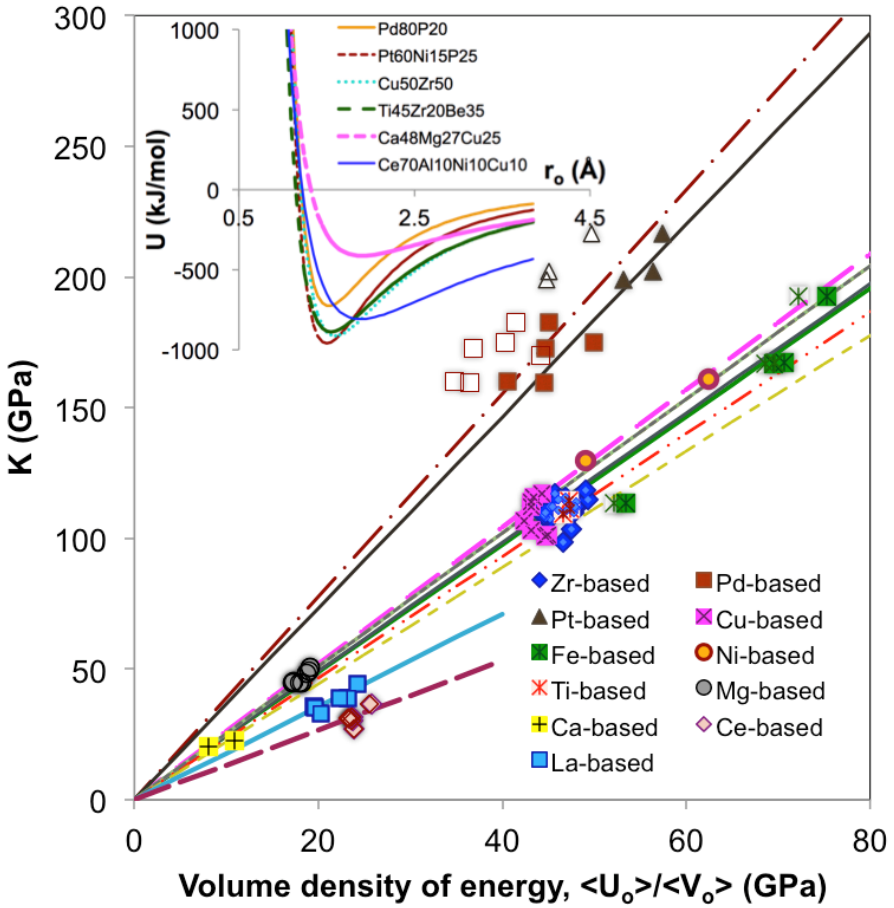
K (GPa)
Volume density of energy, <U$_o$>/<V$_o$> (GPa)
U (kJ/mol)
r$_o$ (Å)
Pd80P20
Pt60Ni15P25
Cu50Zr50
Ti45Zr20Be35
Ca48Mg27Cu25
Ce70Al10Ni10Cu10
Zr-based
Pd-based
Pt-based
Cu-based
Fe-based
Ni-based
Ti-based
Mg-based
Ca-based
Ce-based
La-based

FIG. 5

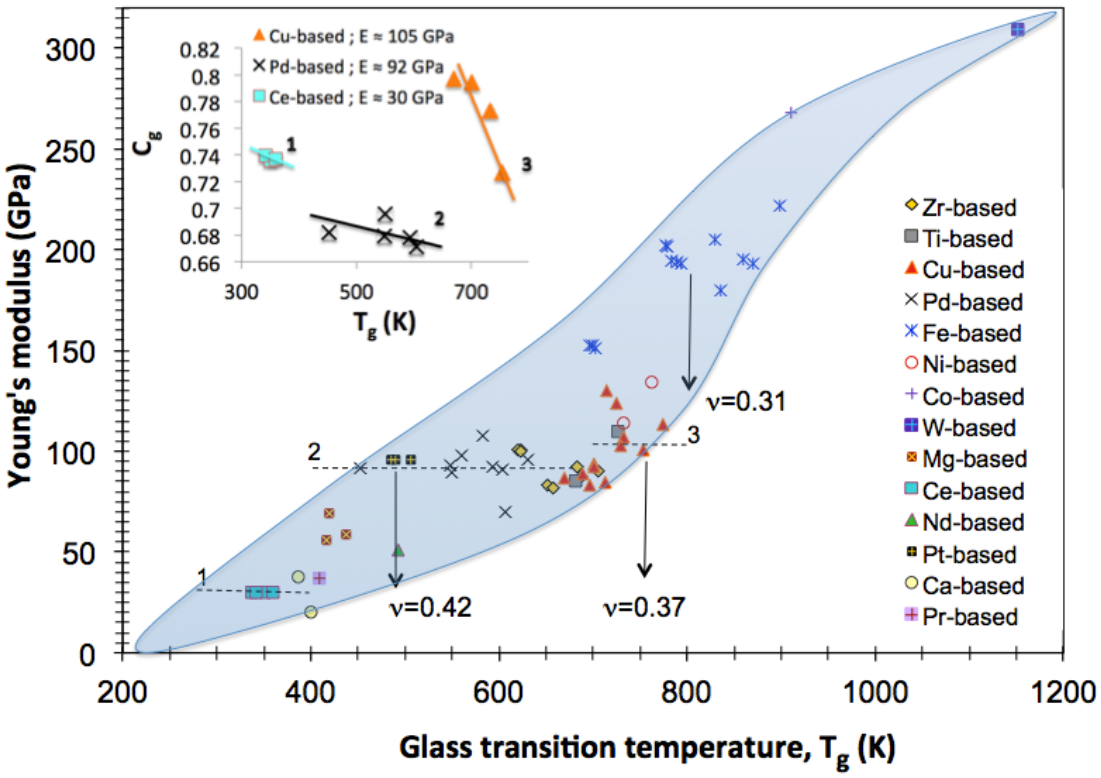
Young's modulus (GPa)
Glass transition temperature, T$_g$ (K)
C$_g$
T$_g$ (K)
Cu-based ; E ≈ 105 GPa
Pd-based ; E ≈ 92 GPa
Ce-based ; E ≈ 30 GPa
ν=0.42
ν=0.37
ν=0.31
Zr-based
Ti-based
Cu-based
Pd-based
Fe-based
Ni-based
Co-based
W-based
Mg-based
Ce-based
Nd-based
Pt-based
Ca-based
Pr-based

FIG. 6